Continental Shelf Research 55 (2013) 141–154

Contents lists available at SciVerse ScienceDirect

Continental Shelf Research

journal homepage: www.elsevier.com/locate/csr

Research papers

A multiproxy study between the Río de la Plata and the adjacent South-western Atlantic inner shelf to assess the sediment footprint of river vs. marine influence

Leticia Burone [a,*], Leonardo Ortega [b], Paula Franco-Fraguas [a], Michel Mahiques [c], Felipe García-Rodriguez [a], Natalia Venturini [a], Yamandú Marin [b], Ernesto Brugnoli [a], Renata Nagai [c], Pablo Muniz [a], Marcia Bícego [c], Rubens Figueira [c], Alexandre Salaroli [c]

[a] Universidad de la República, Facultad de Ciencias—Sección Oceanología, Iguá 4225, Montrevideo 11400, Uruguay
[b] Sección Oceanografía, Departamento de Biología Pesquera, Dirección Nacional de Recursos Acuáticos (DINARA), MGAP, Constituyente 1497, Montevideo, Uruguay
[c] Instituto Oceanográfico da Universidade de São Paulo, Praça do Oceanográfico, 191, 05508-120 São Paulo, SP, Brazil

ARTICLE INFO

Article history:
Received 13 February 2012
Received in revised form
22 December 2012
Accepted 3 January 2013
Available online 23 January 2013

Keywords:
Terrigenous input
Hydrodynamics
Río de la Plata estuary
South-western Atlantic
Inner shelf

ABSTRACT

Proxies of terrigenous versus marine input (Al and Ti, Fe/Ca and Ti/Ca ratios), origin of organic matter ($\delta^{13}C$, $\delta^{15}N$ and C/N ratio), productivity (C_{org}; N_t; $CaCO_3$, P, Ca, and Ba content; and Ba/Al and Ba/Ti ratios), hydrodynamics (grain size, mean diameter and sorting) and biological records of the main features of the environment (benthic foraminifera assemblage distribution) were used to assess the sediment footprint of river vs. marine influence along the salinity gradient between the Rio de la Plata (RdlP) estuary and the adjacent South Western Atlantic Shelf. These criteria permitted characterisation and interpretation of the sedimentary processes influencing transition between three known environments: tidal river, estuarine and marine zones. Increases in sand and clay content at the transition between tidal river and proper estuarine zones indicate resuspension/deposition processes associated with the maximum turbidity zone (MTZ). The MTZ was also characterised by an increase in mixed organic matter content indicated by stable carbon and nitrogen isotope values, an increment in productivity proxies (C_{org}, N_t and $CaCO_3$) and the substitution of the *Miliammina fusca* assemblage (brackish environments) for the *Ammonia tepida* assemblage (estuarine environments). The transition between estuarine and marine environments was characterised by a sharp (up to 99%) increase in sand content, reflecting the progradation of modern RdlP sediments toward relict continental shelf sediment. C/N values typical of the marine environment, decreased trace element concentrations and the distribution of the *Buliminella elegantissima* assemblage (a more marine assemblage) also highlight the marine environment. This paper is particularly important as a tool both to better understand sedimentological dynamics in salinity fronts (along the shelf sediment of large estuaries) and to elaborate more precise palaeoenvironmental and palaeoceanographic reconstructions.

1. Introduction

The physical and biochemical processes that control the depositional environment create an imprint on the final deposited sediment. The close relationship between the depositional process and sedimentary facies and biofacies represents a potential tool for interpreting ancient depositional environments (Boggs, 2005).

On the continental margins, on a regional scale, climatic conditions and hydrological and oceanic regimes are mainly responsible for sediment supply and sedimentation patterns. In addition, the complexity of such processes is increased by the freshwater supply from river discharges. Rivers are the dominant suppliers of particulate material from the land to the sea (globally, ~85–95% of terrigenous discharge is transported by rivers) (Milliman and Meade, 1983; Syvitski et al., 2003; Nittrouer et al., 2007). The largest rivers create extensive deposits near their mouths (e.g., the Amazon, Ganges–Brahmaputra and Mississippi), but the combined discharges of moderate and small rivers dominate the global sediment supply (Nittrouer et al., 2007) and, therefore, are important to the development of continental margin stratigraphy.

A thorough characterisation of the source-to-sink movement of terrigenous sediment is essential to understand the sedimentary record. Moreover, recognition of the major depositional settings (i.e., continental, marginal marine and marine) allows

* Corresponding author. Tel.: +598 2 52 586 18/22.
E-mail addresses: lburone@fcien.edu.uy, lburone@gmail.com (L. Burone).

0278-4343/$ - see front matter © 2013 Elsevier Ltd. All rights reserved.
http://dx.doi.org/10.1016/j.csr.2013.01.003

the inference of environmental and climatic cycles through the Late Quaternary (Hori et al., 2001).

The Rio de la Plata is the second largest fluvial system in South America, draining a catchment area of 35,000 km^2 with an annual water discharge of 22,000 m^3/s and an annual sediment supply of 80×10^6 t/year (Gilberto et al., 2004). Fluvial sediments are first trapped inside the La Plata estuary. A significant passage of sediments is located along the SE Uruguayan coast, following the palaeotopography of the Río de la Plata, with little modern sedimentation over relict continental shelf sediments. However, river plume distribution varies seasonally following the palaeochannel distribution during high river discharge and remaining near and toward the south of the river mouth during the summer season. Thus, modern terrigenous vs. marine-influenced sedimentation along this complex system (tidal river-continental shelf) needs to be evaluated.

Different abiotic and biotic proxies are used to provide information on the average environmental conditions and to assist in the inference and interpretation of the processes responsible for the establishment of particular sediments (Meyers, 1997). Among these, proxies of terrigenous input (Al and Ti levels and Fe/Ca and Ti/Ca ratios) (Arz et al., 1998; Mahiques et al., 2009), the composition of organic matter (δ^{13}C, δ^{15}N and C/N ratio) (Saito et al., 1989; Prahl et al. 1994; Tyson, 1995), productivity (C_{org}; N_t; $CaCO_3$, P, Ca, and Ba content; and Ba/Al and Ba/Ti ratios) (Goldberg and Arrhenius, 1958; Broecker and Peng, 1982; Dymond et al., 1992; Paytan et al., 1993; Paytan and Kastner, 1996, Mahiques et al., 2009), hydrodynamic characteristics (grain-size, mean diameter and sorting) (Gyllencreutz et al., 2010) and the environmental characteristic record (benthic foraminifera assemblage distribution) (Murray, 2006; Burone and Pires-Vanin, 2006) can been used.

The main goal of this work is to assess the sediment footprint of river vs. marine influence in a complex transitional region between the Río de la Plata (RdlP) estuary and the adjacent South Atlantic Shelf using a combination of physical, chemical and biological proxies. Therefore, the information reported in this paper is particularly important to better understand sedimentological dynamics in salinity fronts of large estuaries but also for elaborating more precise data for palaeoenvironmental and palaeoceanographic reconstructions.

2. Study area

The RdlP estuary (Lat. 35°00′–36°10′-S, Long. 55°00′–58°10′W), located in Southeast South America, covers an area of 36×10^3 km^2 and is limited by the Argentinean (south) and Uruguayan (north) coast. The main tributaries are the Paraná and Uruguay rivers, with an annual average discharge of 16,000 and 6000 m^3/s, respectively (CARP, 1989). The RdlP outflow exhibits an average value of 22,000 m^3/s (Framiñan and Brown, 1996) and shows a maximum seasonal variability from March–June and September–October and a minimum from December to March (Guerrero et al., 1997; Nagy et al., 2002).

This river forms a large-scale estuary characterised by a salt-wedge regime; a semidiurnal tide with a low tidal amplitude (<1 m); a broad and permanent connection to the sea; and a high susceptibility to atmospheric forcing due to its large extension and shallowness (Acha et al., 2008, and references therein). The salt wedge river intrusion creates a well-stratified section characterised by two salinity fronts: the bottom salinity front, located in the innermost part of the bottom salt wedge, and the surface salinity front, indicating the transition between the turbid river and the less turbid marine surface waters. The maximum turbidity zone (MTZ), located near the bottom salinity front, is characterised by a high suspended matter concentration associated with deposition and re-suspension processes (Framiñan et al., 2008). Seaward from the surface salinity front, the RdlP buoyant plume outflow modulates salinity distribution over the inner continental shelf and can be traced as a low salinity plume extending as far as 28°S (Piola et al., 2000).

With respect to the geology and geomorphology, the Rio de la Plata is located in the transition zone between the Brazilian shield and the "Pampas" region. As a result, the coastal areas of the RdlP show different characteristics. The north-eastern coast (Uruguay) is formed by low hills where the metamorphic basement of the Brazilian shield outcrops, and low, fluvial-estuarine Holocene environments are only present in reduced strips of the coast (Violante and Parker, 2004). The south-western coast (Argentina) is characterised by extensive, very gently sloping and low-relief coastal plains, developed over underlying Cenozoic deposits, lying 5 m above present sea level (Violante and Parker, 2004).

The area evolved throughout several stages related to different sea level stands during the Late Quaternary, which are represented by the succession of estuarine, fluvial and coastal sedimentary environments (Parker and Violante, 1993; Cavallotto and Violante, 2005). The RdlP is geomorphologically considered one unit (Geomorphological unit 'Rio de la Plata') formed during the Holocene transgression and composed of a set of features genetically linked, which includes the subaerial and subaqueous delta as well as the coastal plains (Cavallotto and Violante, 2005).

Along the subaqueous delta (the bottom of the RdlP water body), the Barra del Indio shoal divides the inner tidal river from the outer estuary proper. The adjacent inner continental shelf constitutes the regional environment affected by the post-LGM transgression (Violante and Parker, 2004).

3. Material and methods

An eleven-station transect (S1 to S11) was created along the RdlP estuary salinity gradient (Fig. 1). The cruise was conducted

Fig. 1. Locations of the study area and sampling sites. The grey shading refers to depth.

during late austral summer (3–9, March) 2008, onboard the R.V. Aldebaran from DINARA (*Dirección Nacional de Recursos Acuáticos*). The stations were each separated by 10 nautical miles (1 nautical mile: 1852 km). The water depth gradient ranged from 5 to 30 m.

Depth, temperature and conductivity profiles of the water column at each station were measured using a CTD cast (SBE-19).

Surface water samples were taken with Niskin bottles. After collection, water samples were filtered through glass fibber filters (Whatman GF/F, 47 mm) to assess total chlorophyll and suspended particulate matter content. Filters were stored dry and frozen for subsequent analysis in the laboratory. Chlorophyll was extracted with 90% acetone and analysed with a Shimadzu UV–2101 PC, UV–VIS Scanning spectrophotometer. The chlorophyll *a* concentration was calculated according to Jeffrey and Humphrey (1975) and modified with a correction for phaeopigments (Lorenzen, 1967). Suspended particulate matter was estimated by the gravimetric method according to Strickland and Parsons (1972). Suspended particulate material, organic matter, chlorophyll *a* and phaeopigment data from stations S1 to S3 were not available due to problems with equipment in the field.

Sediment samples were collected using a Smith–McIntyre bottom grab sampler for the analysis of the following variables: grain size, grain size parameters (mean diameter and sorting), C_{org}, N_t, bulk organic $\delta^{13}C$ and $\delta^{15}N$, $CaCO_3$ content and major and trace elements.

The grain size was analysed using a Malvern Mastersizer 2000 analyser. The carbonate content was determined using the weight difference prior to and after the acidification of 2 g of the sample with a 10% solution of hydrochloric acid. Percentages of 17 intervals (0.5 subclasses) were determined between 9 and -1Φ.

C_{org}, N_t, $\delta^{13}C$ and $\delta^{15}N$ were determined using a Finnigan Delta V Plus coupled with a Costech Elemental Analyser at the Oceanographic Institute of the University of São Paulo, Brazil.

Major (Ti, Al, Fe, Cu, Cr, Ni, Zn, Ca and P) and trace (Ba) element concentrations of bulk sediment were analysed using X-ray fluorescence (XRF) by fused glass discs (FGD) at the Institute of Geosciences of the University of São Paulo, Brazil, following the analytical procedures described in Mori et al. (1999). To check the possible use of Al as a normalising element, Al was plotted against Ti, assuming that Ti is exclusively terrigenous and non-reactive (Mahiques et al., 2009).

Samples to study the benthic foraminifera fauna were taken from the undisturbed sediment recovered by grab sample (a volume of approximately 50 cm^3 per sample). Immediately after sampling, the material was stained with buffered rose Bengal dye (1 g of rose Bengal in 1000 ml of alcohol) for 48 h to differentiate between living and dead foraminifera (Walton, 1952). In the laboratory, the wet samples were carefully washed through 0.250 and 0.062 mm sieves to separate the size fractions. All living specimens in each sample were picked out and identified following the generic classification of Loeblich and Tappan (1988).

Foraminiferal assemblage parameters were calculated. The diversity (H') was calculated on a natural logarithmic basis (ln x) by the Shannon–Wiener index (Shannon and Weawer, 1963). The species richness (S) was determined as the total number of species. The mean diversity ($\overline{H'}$) was obtained according to Burone and Pires-Vanin (2006).

A principal component analysis (PCA) was carried out for the ordination of sampling locations in relation to the environmental gradient. A previously normalised and centred matrix was constructed using the following parameters: C_{org}, N_t, $CaCO_3$, silt, clay, $\delta^{13}C$, $\delta^{15}N$, Ba/Al, Ba/Ti, Fe/Ca and Ti/Ca from the sediment samples and temperature and salinity from the bottom water.

To define groups of stations with similar foraminiferal fauna composition, a non-metric multi-dimensional ordination (nMDS, Kruskal and Wish, 1978) was performed using the density similarity matrix, in which Bray and Curtis (1957) similarity index was employed . The total density was considered for each sample.

To perform uni- and multivariate techniques, we used the multivariate statistical package (MVSP) (Kovach, 1999) and the PRIMER package (version 5.0, Clarke and Warwick, 2001).

4. Results

4.1. Environmental data

4.1.1. Water column

Salinity and temperature data are shown in Fig. 2. The salt wedge could be identified by relatively low salinity values (isohaline of 12) that extend from the bottom at station S1 to the

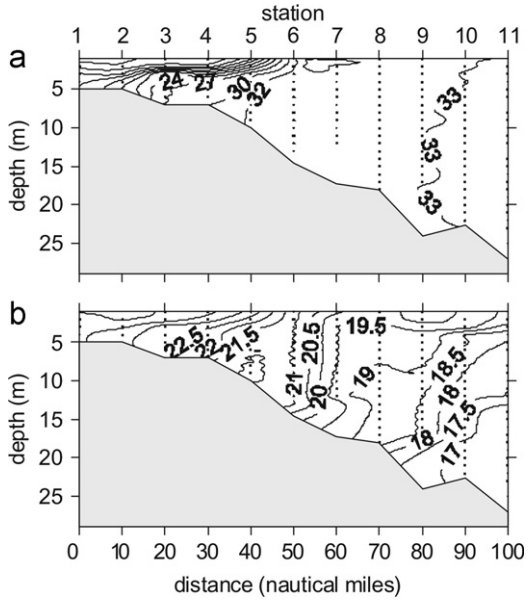

Fig. 2. (A) Salinity profile. (B) Temperature profile. The salinity isohalines are regularly plotted each three units (practical salinity units = PSU) for salinity ≤ 30; isohalines of 32 and 33 were added in order to highlight the higher oceanic influence from S6 to S11.

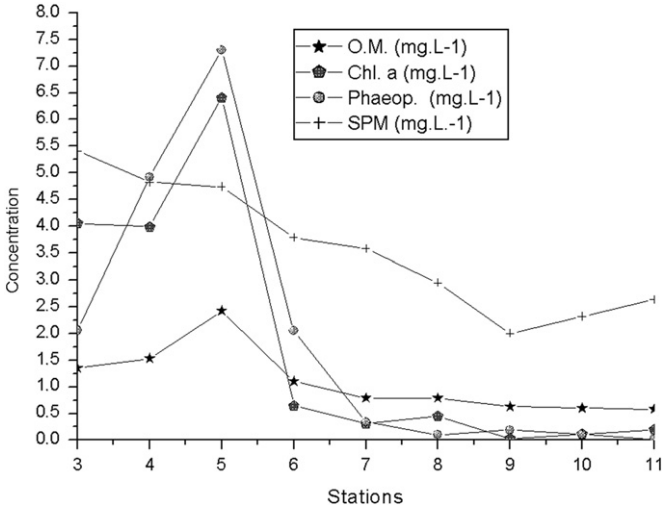

Fig. 3. Parameters measured in the surface water samples: suspended particulate matter (SPM), organic matter (OM), chlorophyll a (Chla) and phaeopigments (Phaeop.).

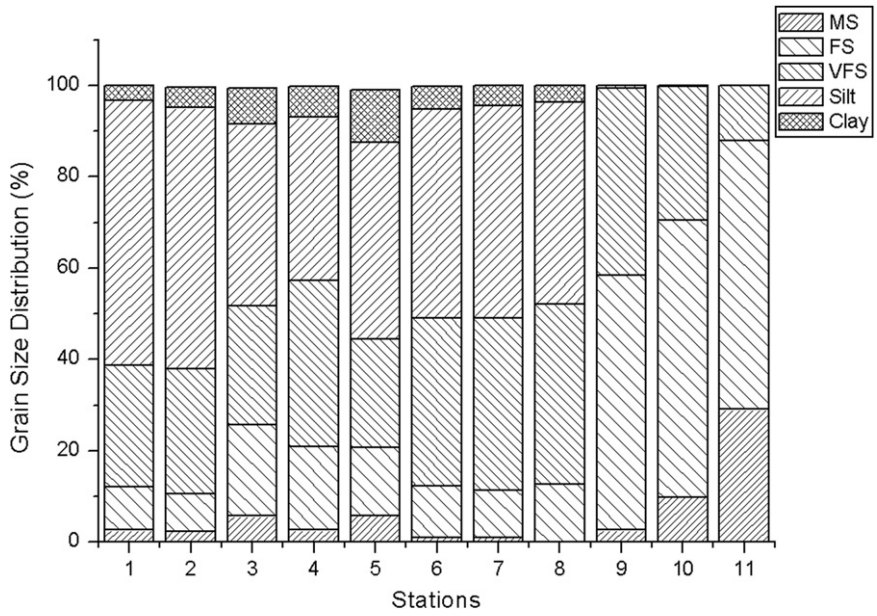

Fig. 4. Relative percentages of the main sediment size fractions in the studied stations. MS=medium sand; FS=fine sand; VFS=very fine sand.

surface of S5. Low-salinity waters (salinity <3) dominate the surface between S1 and S2. The frontal zone includes stations S3, S4 and S5 and exhibits the steepest vertical salinity gradient (reaching up to 23.50). From station S6 to S11, a practically homogeneous marine water column was observed with salinity values of 32 and 33.

The vertical temperature distribution showed a seaward decrease with values between 24 and 19.5 °C in surface waters and between 23.5 and 17.0 °C at the bottom, associated with the dominance of colder oceanic water. The strongest horizontal temperature gradient was observed between stations S5 and S6.

The surface suspended particulate matter (SPM) concentration showed a clear and declining trend toward the outer estuary (except for station S11, where a slight increase was observed). Stations S3–S5 showed the highest values (Fig. 3).

Water column organic matter, chlorophyll *a* and phaeopigments increased from S3 to S5, reaching their maximum at S5 and decreasing seawards (from station 6 to 11) (Fig. 3).

Table 1
Latitude, longitude, depth, mean diameter and sorting in the 11 studied stations.

Station	Latitude	Longitude	Depth (m)	Mean Diam. ϕ	Sorting
1	−34.8584	−56.8903	6.5	4.38	Poorly sorted
2	−34.9052	−56.6850	6	4.52	Poorly sorted
3	−34.9503	−56.4842	7.5	4.41	Very poorly sorted
4	−34.9856	−56.2890	8.2	4.31	Poorly sorted
5	−35.0194	−56.1042	10.5	4.8	Very poorly sorted
6	−35.0531	−55.9073	13.3	4.34	Poorly sorted
7	−35.1006	−55.7088	13	4.27	Poorly sorted
8	−35.1336	−55.5171	20	4.17	Poorly sorted
9	−35.1850	−55.3244	18.7	2.89	Well sorted
10	−35.2178	−55.1171	23	2.7	Medium sorted
11	−35.2543	−54.9015	25	2.33	Medium sorted

4.1.2. Sediment

Grain size (Fig. 4) showed a gradual increasing trend with high percentages of silt and clay from station S1 to S8 (ranging between 48 and 61%) and a sharp increase in sand content eastwards from station S9 (with values between 99.5 and 100%). This coarsening coincided with an increase in water depth (approximately 7 m). Clay was a higher percentage between stations S3 and S5, with the highest values (11.5%) at S5. An increase in medium and fine sand was observed for stations S3 and S5, with values higher than those of the inner stations (S1 and S2) and outer stations (S6–S8). The sediment is poorly sorted between stations S1 and S8 and medium and well sorted from station S9 to S11 (Table 1).

4.1.3. Geochemical proxies

All sediment productivity proxies (C_{org}, N_t, P and $CaCO_3$) had the highest values between stations S3 and S7 (Fig. 5). Values ranged between 0.05 and 1.2% (C_{org}), 0.02 and 0.16% (N_t), 0.05 and 0.1 mg/kg (P) and 5.8 and 22.8% ($CaCO_3$).

A significant positive linear correlation was observed after plotting C_{org} vs. N_t (Fig. 6A). Stations S1 to S7 showed higher C/N values (ranging from 6 to 8) than marine stations (from S8 to S11; ranging from 2.5 to 5) (Fig. 6B). Stable carbon and nitrogen isotope values showed similar trends, increasing from S1 to S8 (from −23.7 to −21.1‰ for $\delta^{13}C$ and from 2.9 to 5.6‰ for $\delta^{15}N$). From S9 to S11, $\delta^{13}C$ values remained in the range of estuarine stations, while $\delta^{15}N$ values decrease (Fig. 7).

The correlation between Al and Ti was statistically significant ($R^2=0.93$, $p\leq 0.05$) and led to the conclusion that Al was terrigenous and non-reactive (Fig. 8A).

Generally, Ti, Al and Fe presented a decreasing seaward gradient (Fig. 8B–D). However, a slight increase in both elements was observed in stations S5–S7. A conspicuous decrease in the values of these elements was observed from S7 to S11, reaching their minimum value at station S11. The same trend was observed in the other elements such as Zn, Cr and Ni (Fig. 8E–G) and in Ti/Ca and Fe/Ca ratios (Fig. 9). Consequently, the inverse behaviour was observed for the Ba/Al ratio, which showed an increased seaward gradient (Fig. 9).

As expected, silt and clay fractions exhibited significant positive correlations with Fe, Al, Zn, Cr, Ni, Cu, C_{org} and N_t (Table 2). Ti had significant positive correlations with Al, Zn, Cr and Ni but significant negative correlations with Ca and Ba, reinforcing its terrigenous character.

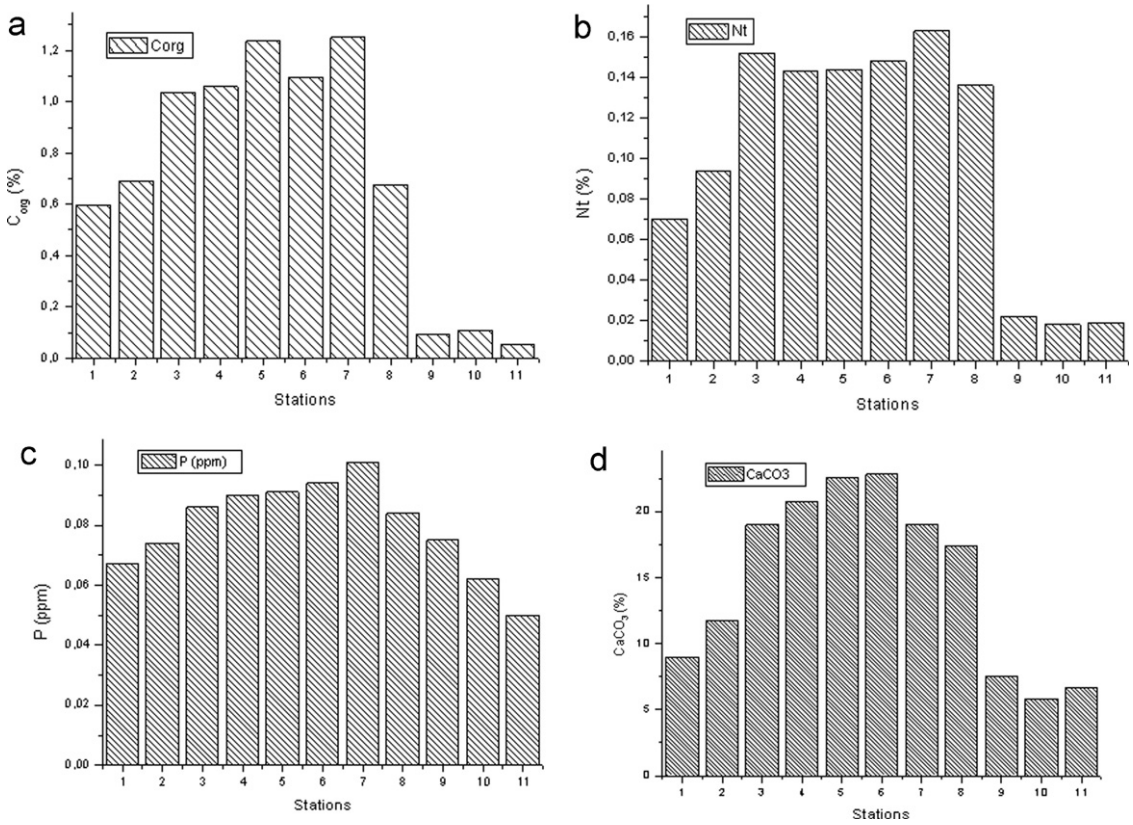

Fig. 5. Organic Carbon (C_{org}), total Nitrogen (N_t), Phosphorous (P) and $CaCO_3$ percentages in the studied stations.

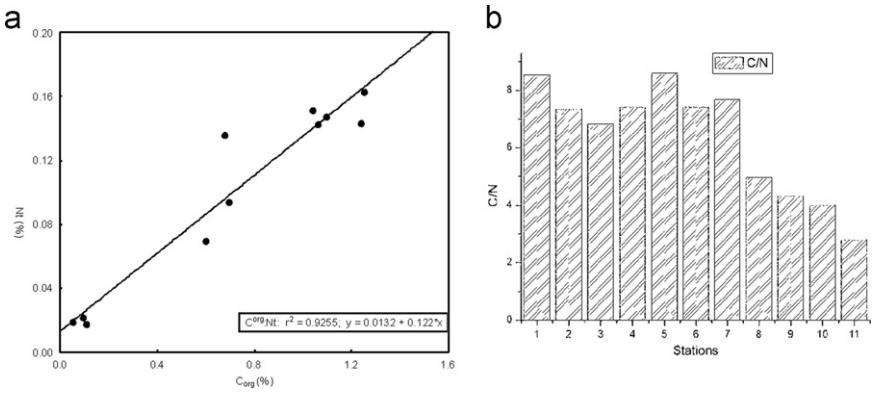

Fig. 6. (A) Linear regression of the C_{org} and N_t contents for the sediment samples and (B) C/N ratio distribution.

4.1.4. Principal component analysis (PCA)

The PCA differentiated the four main groups of sampling stations (Fig. 10). The first and second components together explained 84.46% of the total data variance (with 65.5% explained by the first component).

Group 1 was positively related to Axis II due to the high Ti/Ca, Fe/Ca and temperature values and the relatively high silt percentage in the sediment. Group 2 was negatively linked with Axis I due to the high concentration of C_{org}, N_t, P, $\delta^{15}N$, $CaCO_3$ and the muddy fraction. Group 3 was positively related to Axis II due to the sharp changes that the environmental variables created at this station; high salinity and $\delta^{13}C$ were observed.

However, Group 4 was negatively linked with Axis I due to high values of Ba/Al, Ba/Ti and fine and medium sand.

4.2. Biotic data

4.2.1. Fauna

A total of 51 species of living benthic foraminifera (Table 3) that belong to the suborders Rotaliina (36 species), Textulariina (10 species) and Miliolina (5 species) were registered. Additionally, two species of the order Thecolobosa were recorded.

4.2.2. Non metric dimensional scaling (nMDS) ordination

The nMDS ordination analysis recognised three foraminiferal assemblages, which highlighted the presence of an environmental gradient (Fig. 11). The *Miliammina fusca* assemblage (composed

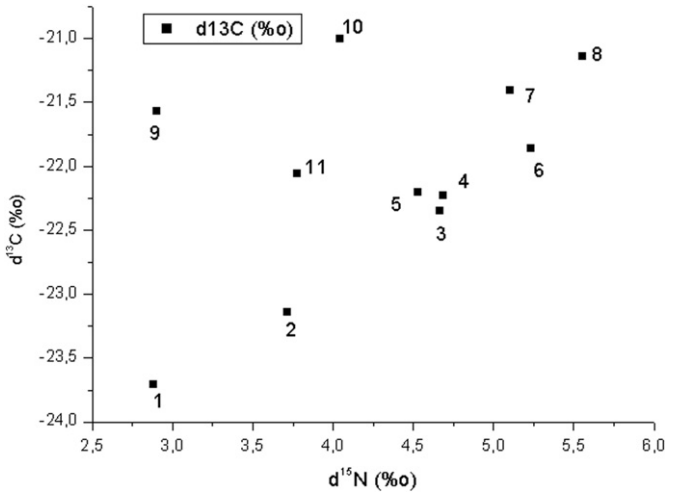

Fig. 7. Plotting of $\delta^{13}C$ (‰) vs. $\delta^{15}N$ (‰).

by the *M. fusca* and *Ammonia tepida* species and two thecamoebian species) is distributed in the more riverine S1, S2, S3 and S4 stations.

The assemblage *A. tepida* included 14 hyaline species represented by *A. tepida*, *Bolivina* spp., *Buliminella elegantissima*, *Hopkinsina pacifica* and *Pseudononion atlanticum*, the porcelanoid species *Quinqueloculina milletti*, 4 agglutinant species and one thecamoebian species. This assemblage was distributed at stations S6–S8.

Finally, the *B. elegantissima* assemblage was distributed in the outermost stations (S9–S11) and showed the highest number of species. Additionally, the presence of species that typically inhabit shelf environments (i.e., *Labrospira* sp., *Poroeponides lateralis*, *Nonion* sp. and *Pyrgo* sp.) was observed.

Station S5 did not appear as part of any group due to the high density of the microgastropod *Heleobia australis*.

4.2.3. Foraminiferal density, diversity and richness

The density (D), diversity (H') and richness (S) values are presented in Fig. 12.

A clear seaward increase for the three studied indexes was observed.

5. Discussion

The spatial distribution of surface sediment and its geochemical characteristics reveal the existence of different sediment facies, which are strongly correlated with the source of the sediments and hydrological conditions and the evolution of climatic and sea level change in the region (Mahiques et al., 2004). These environmental characteristics are also reflected in the composition of the benthic foraminiferal assemblages (Scott et al., 2001; Burone and Pires-Vanin, 2006). In this study, the sediment proxies analysed reflect the RdlP, estuary and adjacent Atlantic inner shelf environmental conditions.

5.1. Environment description based on water proxies

According to Cabreira et al. (2006), the RdlP estuary is typically a two-layer system with a salt wedge the majority of the time and freshwater flows seaward over the surface. The inner part of the estuary has a strong salinity stratification, while a lower gradient characterises the surface salinity front. In addition, a well-developed turbidity front characterises the innermost part of the estuary (Framiñan and Brown, 1996; Framiñan et al., 2008). This front, located near the bottom salinity front, is where a large portion of the transported solids flocculate due to the opposing river discharge, incoming tide and wave and tidal current resuspension processes (Parker et al., 1987; López-Laborde and Nagy, 1999; Cavallotto and Violante, 2005; Framiñan et al., 2008). As expressed by Acha et al. (2008), high turbidity constrains photosynthesis in the estuary, but immediately offshore of the turbidity front, water becomes less turbid and phytoplankton peaks. Consequently, the consumption of available nitrogen inside the estuary results in a decrease in productivity seaward (Acha et al., 2008).

In this study, the water column salinity permits the recognition of the salt wedge edge up to the innermost station (S1) and shows the steepest salinity gradient between S3 and S5. Additionally, the turbidity front position and transition to ocean mixed waters are reflected in the suspended particulate matter, organic matter concentration, chlorophyll *a*, and phaeopigment values from the surface water. Although data are not available from the entire water column and from surface water in stations S1 and S2, a maximum suspended particulate matter was observed in S3, and the decrease seawards presumably indicates the turbidity front position. This postulate is supported by the high chlorophyll *a* values observed between S3 and S5, with a peak in chlorophyll *a*, organic matter concentration and phaeopigments in S5, followed by a sharp decrease seaward.

The salinity front varies in time and space and summer prevailing onshore winds, and a minimal river runoff induces higher salinity levels (Framiñan and Brown, 1996; Gómez-Erache et al., 2001; Nagy et al., 2002). The observed turbidity front position agrees with a study of Framiñan and Brown (1996). These authors used a four year span of National Oceanic and Atmospheric Administration's-Advanced Very High Resolution Radiometer (NOAA-AVHRR) daily images to determine that the front position varies between 57°00′ and 54°12′W.

Thus, the turbidity front position (S3, Table 1) presents an anomalously inward position. This discrepancy could be associated with the strong La Niña event that occurred in 2008 (http://www.cpc.ncep.noaa.gov/products/analysis_monitoring/ensostuff/ensoyears.shtm). The El Niño/La Niña-Southern Oscillation (ENSO) has a well-documented impact on precipitation in the RdlP basin during austral spring (October–December) and in fall–winter (March–July) (Pisciottano et al., 1994; Diaz et al., 1998; Robertson and Mechoso, 1998; Cazes-Boezio et al., 2003), tending to be below (above) the median in cold (warm) events. The Uruguay and the Negro River flows show a characteristic ENSO-like pattern, with above average discharge coinciding with the warm phase (Mechoso and Perez-Iribarren, 1992; Robertson and Mechoso, 1998). Although the Parana River exhibits some variability on ENSO timescales (Depetris et al., 1996), the spectrum is dominated by a longer period of variability (Robertson and Mechoso, 1998). The anomalously inward position of the RdlP turbidity front (between ~56 and 56.5°W) in March 2008 reflects lower precipitation over the RdlP drainage basin and reduced river input during a La Niña interval.

5.2. Sediment environmental footprint

5.2.1. Grain size distribution

Although biogenic opal was not removed before grain-size measurements, its potential influence on the sediment grain size data may be neglected (Romero and Hansen, 2002; Frenz et al., 2003). These authors showed that surface sediments from the Southwestern Atlantic Ocean contained a very low ($<1.3\%$) biogenic opal content. Therefore, the biogenic opal influence can be minimised in the sand/silt/clay relations, and the sediments

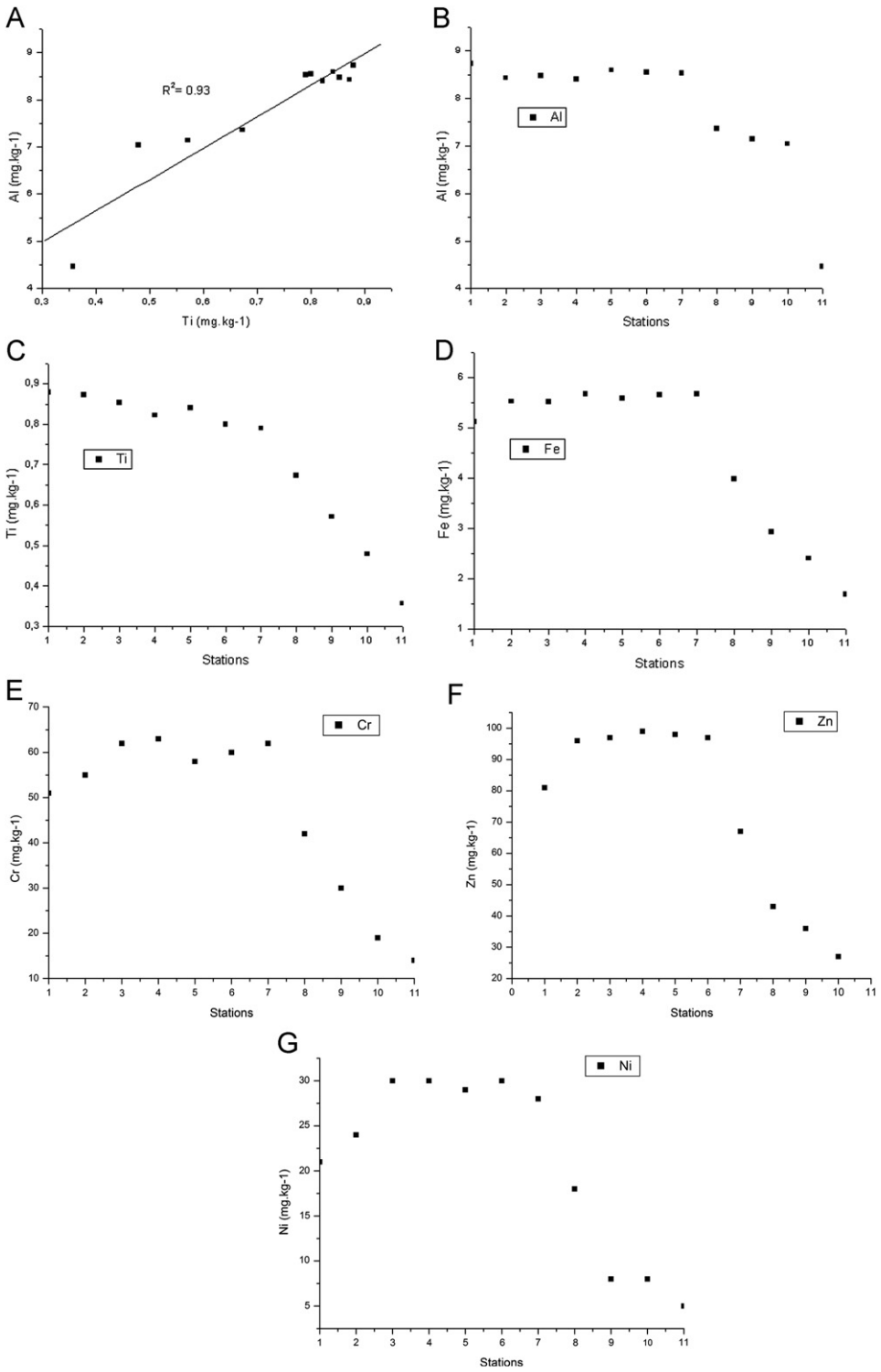

Fig. 8. (A) Linear regression of the Al vs. Ti concentrations; Dispersion plots of (B) Al vs. stations; (C) Ti vs. stations; (D) Fe vs. stations; (E) Cr vs. stations; (F) Zn vs. stations and (G) Ni vs. stations.

can be assumed to consist of only biogenic carbonate and terrigenous components.

From a geomorphological point of view, the subaqueous delta of the RdlP extends from the subaerial delta front to the prodelta, which is located at the transition to the continental shelf (Cavallotto, 2002). While subaqueous fine sediments are in present hydrodynamic equilibrium, sandy continental shelf sediments are not, due to the different hydraulic deposition regime; modern RdlP sediments prograde on top of relict continental shelf sediments (Urien and Ewing, 1974; Lopez-Laborde, 1987; Cavallotto, 2002). The seaward increase in sediment grain size most likely reflects this process and agrees with previous studies (Urien and Ewing, 1974; Lopez-Laborde, 1987; Martins et al., 2003), which describe arcs of increasing grain size sediments (sandy silt and silty sand to sandy shelf) indicating progradation of RdlP sediments upon the continental shelf. The sharp textural increase (up to 99% sand) observed from S9 to S11 indicates the seaward limit of modern dispersion of RdlP

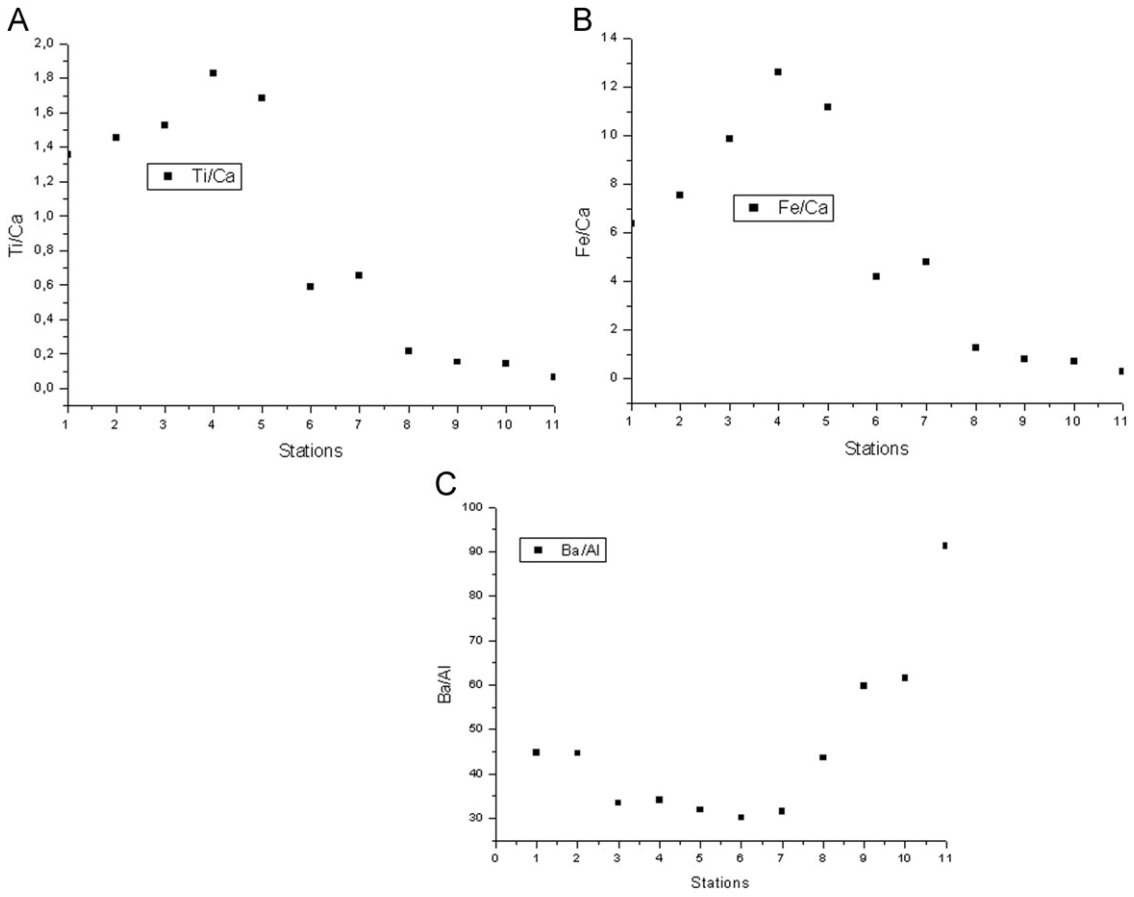

Fig. 9. Dispersion plots of (A) Ti/Ca vs. stations; (B) Fe/Ca and (C) Ba/Al.

Table 2
Pearson correlation. Significant values in bold ($p < 0.05$). MS=medium sand; FS=fine sand and VFS=very fine sand; C_{org}=organic carbon.

	Al	Fe	Ti	Zn	Cr	Ni	Ba	Ca	C_{org}	N_t
Al	1.00	**0.89**	**0.75**	**0.85**	**0.83**	**0.83**	**−0.77**	**−0.78**	**0.83**	**0.80**
Ti	**0.93**	**0.88**	1.00	**0.91**	**0.95**	**0.90**	**−0.64**	**−0.97**	**0.81**	**0.75**
Silt	**0.71**	**0.83**	**0.75**	**0.85**	**0.80**	**0.86**	**−0.80**	**−0.78**	**0.76**	**0.74**
Clay	0.54	**0.82**	**0.91**	**0.82**	**0.84**	**0.81**	**−0.61**	**−0.82**	**0.86**	**0.80**
MS	**−0.79**	**−0.67**	**−0.73**	**−0.69**	**−0.69**	**−0.60**	0.43	**0.67**	**−0.55**	−0.57
FS	**−0.62**	**−0.84**	**−0.91**	**−0.88**	**−0.89**	**−0.87**	**0.72**	**0.82**	**−0.83**	**−0.84**
VFS	0.59	0.36	0.26	0.28	0.33	0.24	−0.26	−0.20	0.25	0.34

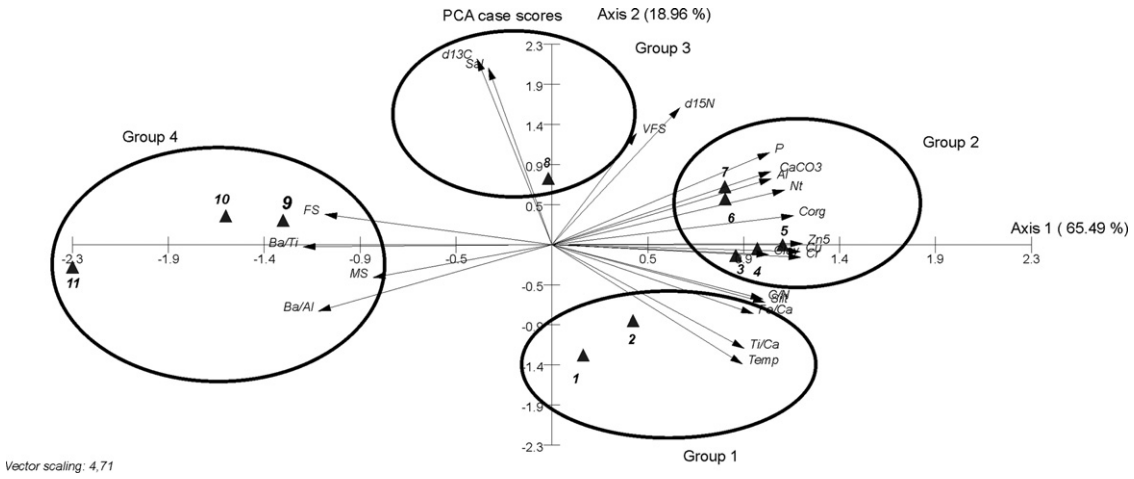

Fig. 10. PCA ordination diagram of sampling based on the selected variables. The four main groups are shown (Group 1–4).

Table 3
Absolute abundance of foraminifera species present in each estudied station.

Stations/species	1	2	3	4	5	6	7	8	9	10	11
Ammonia tepida		18	5	59	4	63	58	28		2	
Ammonia parkinsoniana		6	1	1							
Ammonia roulshauseni								4			
Bathysiphon sp.										4	
Bolivina compacta					1			6		1	13
Bolivina tortuosa											2
Bolivina sp.						4	12		14	4	
Bolivina sp_2.							12	2	12		18
Bolivina sp_3.							1		2	1	6
Bolivina sp_4.								3		1	
Brizalina fragilis										1	8
Bucella peruviana								1	2		1
Bulimina marginata									3		2
Buliminella elegantissima						2	18	5	90	69	52
Cibicides sp.											1
Cibicides lobatulus											1
Cibicidoides sp.										1	
Discorbis floridanus											3
Discorbis williamsoni											14
Elphidium discoidale											20
Elphidium excavatum		2									
Geminospira sp.										1	
Globocassidulina minuta								1			2
Guttulina sp.									2		
Haynesina sp.		1							1		
Hopkinsina pacifica							22	4	4	1	6
Labrospira sp.											14
Lagena laevis											3
Marsipella sp.											5
Massilina sp.									1		
Miliammina fusca		13									
Nonion sp.						1		3	9	1	6
Nonionoides auris								48		10	16
Oolina sp.											1
Operculina sp.											1
Poroeponides lateralis											3
Psammosphaera sp.			1	1							
Pseudononion atlanticum							7	18		8	1
Pyrgo sp_1											1
Pyrgo sp_2.											1
Quinqueloculina atlantica											9
Quinqueloculina milletti						5	14	63	3	2	34
Robertina sp.								6			
Saccammina atlantica										37	12
Sigmoilopsis schlumbergeri											3
Spiroloculina depressa											
Textularia candeiana						2			9		
Textularia earlandy								2			
Triloculina trigonula											1
Trochammina ochracea											1
Virgulina rigii								3			
No identified species							2				
Thecamoebians											
Sp_1.	19	79	6				4	19			
Sp_2.		2	5	2							
Microgasteropod											
Heleobia cf. australis		16	18	50	41						

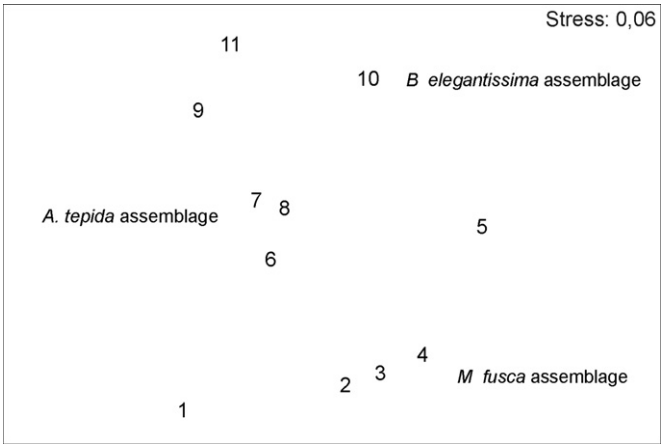

Fig. 11. nMDS ordinations of the stations. Stress of the dimensional configuration (0.06) is shown.

sediments (Urien et al., 1980; Martins et al., 2003; Ayup-Zouain, 2006). These authors describe a sandy belt that covers the middle shelf, which is characterised by a high percentage (between 80 and 90%) of fine sand and an average mean diameter of 1.8ϕ. These relict sediments, deposited and reworked during the Late Pleistocene–Holocene sea level changes (Urien and Ewing, 1974), are well sorted, which is in agreement with the present results. Accordingly, the sharp bathymetric change observed from station S7 to S11 is associated with the RdlP palaeovalley limit (Urien et al., 1980; Cavallotto, 2002; Ayup-Zouain, 2006).

This limited dispersion of modern RdlP sediments is controlled by trapping of suspended sediments in the maximum turbidity zone (MTZ) (Framiñan and Brown, 1996; Framiñan et al., 2008). In general, convergent transport, stratification of the water column, flocculation and resuspension processes characterise the MTZ (Traykovski et al., 2004; Framiñan et al., 2008). In other estuaries, several authors determined subsequent deposition and erosion of sediments in the MTZ associated with ebb and flood tidal phases (Gibbs et al., 1989; Geyer, 1993; Lick and Huang, 1993; Jaeger and Nittrouer, 1995; Traykovski et al., 2004). Deposition of fine porous sediments and resuspension of the finest particles leave behind silt and very fine-grained sand beds. Thus, if the supply of sediment to this trapping region is greater than the amount that can be resuspended, deposits will form under the maximum estuarine turbidity (MET) (Wellershaus, 1981). In tidal environments, these deposits reflect the variations in tidal energy through sedimentary structures known as tidal rhythmites or tidalites, which are alternating beds of fine sand, silt and mud that may appear homogeneous or internally laminated (Traykovski et al., 2004).

In the RdlP, the MTZ is associated with the Barra del Indio shoal (Fig. 1), which based on its morphology and dynamics, divides the inner tidal river with the outer estuary proper (Framiñan and Brown, 1996). In addition to seasonal discharge-related control, variation of the RdlP's MTZ is highly variable on short time scales associated with tides, winds and storms (Framiñan et al., 2008). Therefore, the slight increase in medium and fine sand observed between stations S3 and S5 and the increased clay in S5 may reflect local sedimentary processes associated with MTZ. Moreover, tidal resuspension may explain the relatively low percentage of clay observed in the sediment (maximum value of 11%) compared to previously reported maximum turbidity values in the RdlP estuary ($>25\%$) (Urien, 1967).

5.2.2. Distribution and composition of organic matter

As expected, the frontal zone exhibits high C_{org} and N_t content as well as P values (Fig. 5). The significant positive correlation between muddy sediment and organic matter is favoured by the similar settling mechanism that involves both particulate organic constituents and fine-grained mineral particles (Tyson, 1995). Nevertheless, higher values of C_{org}, N_t and P can been observed until reaching S7, following the silt distribution (Figs. 5 and 4). This finding may reflect both flocculation processes and high productivity associated with the frontal zone.

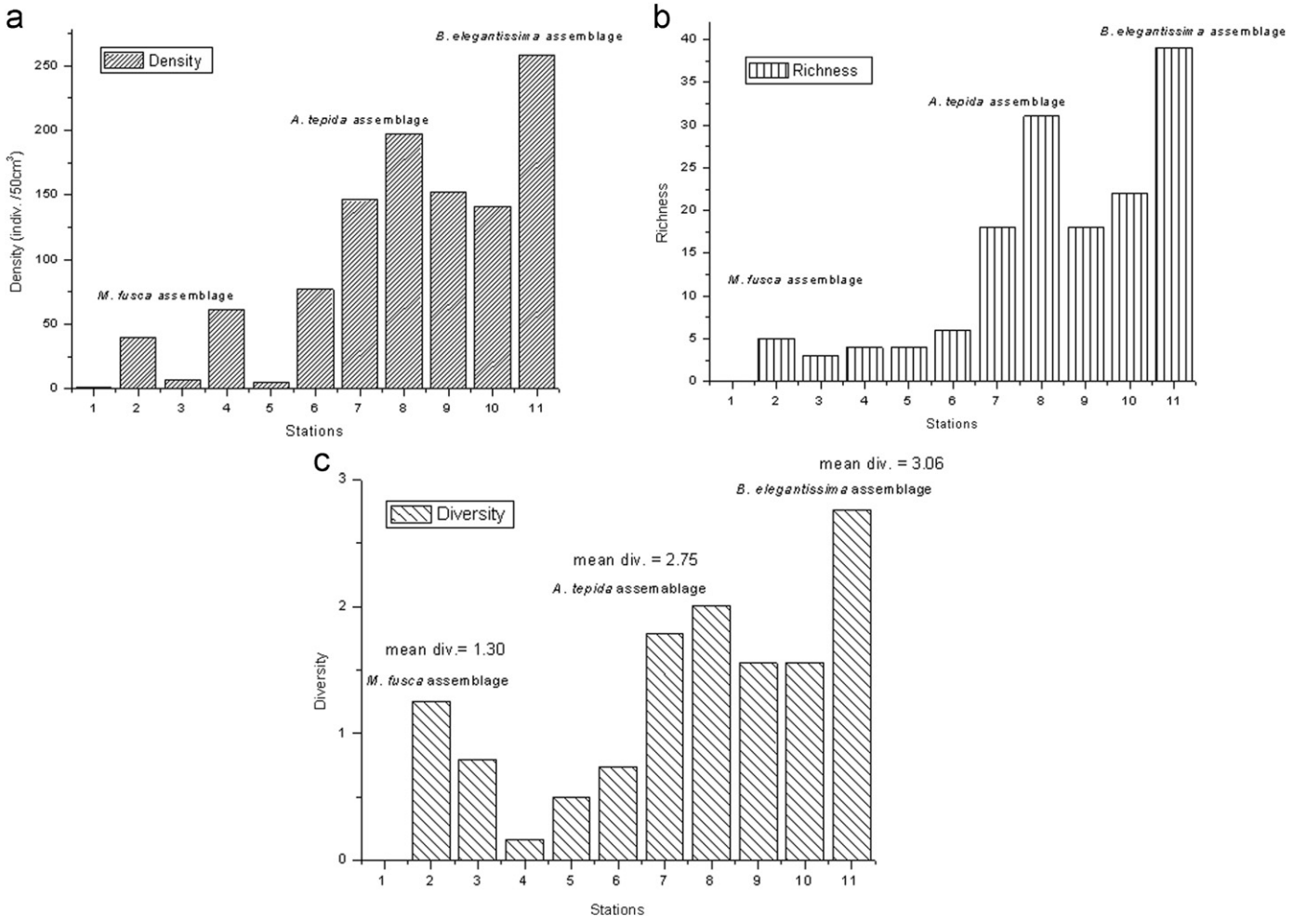

Fig. 12. Biological parameters used to relate the foraminiferal assemblages to the environmental conditions; (A) density; (B) richness and (C) diversity.

The sharp decrease in C_{org}, N_t and P from S7 to S11 (Fig. 5) reflects the decrease in productivity seaward from the turbidity front and the off shoreward dispersion of modern sediments along the estuary. The $CaCO_3$ content distribution was similar to sediment organic matter distribution with higher values between S3 and S7 (Fig. 5) reflecting benthic productivity associated with food availability along the frontal zone (Acha et al., 2008).

The C/N ratio, $\delta^{13}C$ and $\delta^{15}N$ have been used for decades as parameters for evaluation of the relative influence of terrestrial and marine organic matter (Meyers, 1994, 1997; Müller and Mathesius, 1999; Kuramoto and Minagawa, 2001). Moreover, stable carbon and nitrogen isotopes are widely used in food web studies (Rodriguez-Graña et al., 2008).

Several authors suggested different values of C/N ratios according to the origin of the organic matter. Saito et al. (1989) has suggested that a ratio higher than 20 is indicative of a terrestrial origin and between 5 and 7 of a pelagic source. In addition, Stein (1991) reported that values of the C/N ratio lower than 10 are indicative of a strict marine origin and that values of approximately 10 represent both marine and terrestrial organic components in the sediment. Botto et al. (2011) observed relatively low C/N values (10.5) in freshwater marsh macrodetritus from sediments in the RdlP maximum turbidity zone. These authors suggested that this detritus is highly decomposed when it reaches the water. Taking this possibility into account, the C/N ratios observed in the surface sediments of the study area seem to reflect a mixed origin of the organic matter between stations S1 and S7 and a clear marine organic component from station S8 to S11 (see Fig. 6).

When analysing margin sediments from Washington (USA), Prahl et al. (1994) determined that values of $\delta^{13}C = -27.8‰$ were terrestrial and $\delta^{13}C = -20.1‰$ were marine (and these values represented the end-members for these parameters). Typical $\delta^{15}N$ values average ~3 and 6‰ for terrestrial plants and marine particulate organic carbon, respectively (POM; Wada and Hattori, 1991; Muller and Voss, 1999; Maksymowska et al., 2000). The systematic increase in both the carbon and nitrogen stable isotope sediment signal along the estuary (from S1 to S8, see Fig. 7) indicates a mixed origin of organic matter and reflects the increased seaward contribution of marine versus terrestrial detritus. Thus, stable isotope proxies appear more accurate than C/N values in the identification of the relative contribution of terrestrial and marine organic matter sources in the RdlP estuary. These results agree with Botto et al. (2011) and are based on RdlP maximum turbidity, POM and freshwater marshes from the Argentinean RdlP coast, and the appointed contribution of both phytoplankton and terrestrial detritus to this area.

A decrease in nitrogen stable isotope values and maintenance of estuarine carbon isotope values in oceanward stations (S8–S11, Fig. 7) may reflect the lateral influence of stable isotope terrestrial detritus from Uruguayan coastal lagoons, and Solis and Maldonado semi-estuarine complexes. However, C/N values do not reflect this contribution. The presence of inorganic nitrogen in low organic matter sediments (as observed in these stations)

could explain the decrease in stable nitrogen isotopes (Meyers, 1997; Hu et al., 2006). Despite these findings, organic carbon versus total nitrogen values (intercept=0.01, Fig. 6) indicate a contribution of organic nitrogen in these samples. Alternatively, this decrease could be result of a change in the type or size of primary producers at marine stations (Michener and Kaufman, 2007). In summary, while C/N values permit the identification river–estuarine from marine stations, river and estuarine stations are distinguished by means of stable isotopes. This result confirms the importance of working with a multiproxy approach.

Based on high C/N and $\delta^{13}C$ values of POM, Botto et al. (2011) suggested a contribution of salt marsh detritus to the RdlP Argentinean mixohaline coast. Our results suggest that salt marsh detritus does not show a significant contribution. These data are relevant for food web studies along the estuary gradient.

5.2.3. Major and trace elements

All of the chemical elements analysed in this work except Ca and Ba (i.e., Ti, Al, Fe, Cu, Cr, Ni and Zn) are related to terrigenous inputs. From the plot of Al against Ti (Fig. 8), the predominant source of Al was assumed to be lithogenic and non-reactive. The highest values of Al were observed at stations S5–S7 and associated with the pelitic sediments (Fig. 8B). According to Araujo et al. (2002) and Martins et al. (2007), this element is mainly associated with finer sediment fractions (phyllosilicates), which remain in suspension longer and are easily resuspended.

All of the chemical elements mentioned above show a positive linear correlation to Ti (Table 2). According to Martins et al. (2007), these elements could have been supplied by rivers in an adsorbed manner on sediment fine particles, mainly in clay minerals due to their higher specific surface areas available for metal adsorption. This theory explains why the highest values observed occurred between stations S3 and S7 (Fig. 8).

The input of terrigenous versus marine material can also be evaluated by utilising the ratios of Fe/Ca and Ti/Ca (Adegbie et al., 2003; Jaeschke et al., 2007; Govin et al., 2012). Variations in these ratios can be interpreted as changes in continental input, but only in regions where changes in carbonate content are very small (Arz et al., 1998; Jaeschke et al., 2007). Although our carbonate data indicate $CaCO_3$ variations along the transect up to 20%, this variation enhances the results obtained using the elemental ratios. The increase in Fe/Ca and Ti/Ca values between stations S1 and S5 (Fig. 9A) likely reflects the increased input of terrigenous material related to the turbidity zone (despite the increase in $CaCO_3$) (Fig. 5D). The low Fe/Ca and Ti/Ca values between stations S6 and S11 indicate the strong reduction in continental input relative to marine carbonate production (despite the decrease in $CaCO_3$) (Fig. 5D).

This zonal differentiation can be confirmed by the PCA groups (Fig. 10). These groups correspond with the more riverine zone (S1 and S2), the frontal zone (S3–S7), the limit of the estuary (S8) and the marine zone (S9–S11).

Ba is one of the most widely used proxies for estimating marine palaeoproductivity (Dymond et al., 1992; Paytan and Kastner, 1996, Combes et al., 1999, 2005; Calvert and Fontugne, 2001; Pfeifer et al., 2001;Prakash Babu et al., 2002; Wei et al., 2003). Thus, to know its distribution in recent sediments is extremely important. Because there is no regional background Ba value, the total Ba values (biogenic barium+terrigenous barium) were considered. Nevertheless, the Ba/Al ratio reflects marine versus terrigenous input: low Ba/Al values between stations S1 to S7 suggest the dominance of continental input in the RdlP estuarine zone, whereas high Ba/Al values between stations S8 to S11 indicate a decrease in continental versus marine input (reflecting more marine conditions) (Fig. 9).

5.3. Benthic foraminifera

According to Scott et al. (2001), identifying marine-freshwater transitions in the geological record requires familiarity with the fossilisable biota present in modern marginal marine environments.

In our study area, the foraminiferal and thecamoebian associations appear strongly structured by the environmental characteristics, indicating a strong gradient from fresh to marine water. The *M. fusca* association is distributed in the more riverine stations and is characterised by a reduced number of species, low mean diversity, low density and the presence of thecamoebians (Figs. 11 and 12). *M. fusca* is a species typical of very low-salinity waters (Scott et al., 2001) and has already been found in many Brazilian river–estuarine environments (Zaninetti et al., 1979; Brönniman et al., 1981; Bonetti and Eichler, 1997; Burone and Pires-Vanin, 2006; Mahiques et al., 2010). The ecological attributes of this assemblage, associated with the absence of typical marine species, reflect the strong influence of fresh water input in this zone and are documented by the abiotic proxies analysed.

From station S6 to S8, the *M. fusca* assemblage is replaced by the *A. tepida* assemblage. *A. tepida* is considered to be a mixohaline species with a high ability to tolerate abrupt salinity changes (Walton and Sloan, 1990; Burone and Pires-Vanin, 2006; Burone et al., 2006; Burone et al., 2007). Furthermore, Debenay et al. (2001) state that the growth of *A. tepida* may be favoured by a temporal decrease in water salinity and inputs of nutrients, which occur in this region. Nutrients are usually involved in an increase in primary producers (microalgae), which results in an important feeding source of herbivore foraminiferal fauna such as *A. tepida*, as observed by Burone and Pires-Vanin (2006). The assemblage is also composed of infaunal deposit-feeder species such as: *Bolivina* spp., *Nonionoides* spp., *P. atlanticum* and *B. elegantissima* (Murray, 2006) that are related to the high mud, carbon, phosphorous and nitrogen values observed. From an ecological point of view, this association is characterised by average diversity and density values and marks an intermediate environment (estuarine conditions).

It is important to note that station S5 appears isolated in the nMDS (Fig. 11; it is not represented by any assemblage) due to the low density of foraminifera and high density of the microgastropod *Heleobia cf. australis*. The negative foraminiferal response in this station may be correlated to the stressful environmental conditions. Frontal systems (stratified systems, the majority of the time) are highly susceptible to oxygen stress below the halocline as a response to nutrient over-enrichment and the consequent increase of productivity and organic matter respiration (Diaz and Rosenberg, 1995). Rabalais et al. (1996) showed how high nitrogen input and saline stratification associated with the Mississippi river discharge increased primary production rates and extended hypoxic areas in the Gulf of Mexico. Furthermore, the presence of *H. cf. australis* was already discussed. This result was confirmed by a macrofauna distribution study conducted in the same gradient that showed the dominance of this opportunistic species at station S5 (unpublished data). It is important to note that this species is extremely resistant to organic-enriched and oxygen-depleted environments (Muniz et al., 2005; Muniz et al., 2011), most likely occupying niches that could not be colonised by foraminifera species.

Finally, the *B. elegantissima* assemblage, composed of more marine species typical of shelf environments (Murray, 2006; Burone et al., 2007) and showing the highest number of species,

mean density and mean diversity values, clearly reflects the marine conditions prevailing in the outermost stations.

6. Final considerations

This work is based on a multiproxy approach applied for the first time along the environmental gradient from the Río de la Plata to the South Atlantic Ocean.

Sediment biogeochemical proxies permitted characterisation and interpretation of sedimentary processes influencing transition between three known environments: tidal river, the estuarine zone and the marine environment. Water column, physical (temperature and salinity) and geochemical (grain-size variations, organic carbon, trace and major elements, stable isotopes and $CaCO_3$ percentages) data were used as environmental controls for sediment characterisation.

The increased content of sand (c.a. 20%) and clay (c.a. 10%) (S3–S5) in an otherwise muddy environment (S1–S7) indicates resuspension/deposition processes associated with the maximum turbidity zone (MTZ). This information assisted in identification of the transition between the tidal river (S1 and S2) and the estuary proper (S3 to S7). Additionally, an increase in mixed organic matter influence is indicated by a systematic increase in stable isotopes ($\delta^{13}C$ and $\delta^{15}N$) and a two-fold (c.a. 50%) increase in productivity (C_{org}, N_t and $CaCO_3$ proxies). A slight increase (c.a. 17%) in trace elements (principally in Cr, Zn and Ni) and a sharp (30–50%) increase in Ti/Ca and Fe/Ca proxies indicates enhanced continental material associated with frontal turbidity processes. A shift occurred from the *M. fusca* assemblage characterised by low richness, diversity and density values to the *A. tepida* assemblage composed of euribiontic species typical of estuarine environments.

A sharp increase in sand content (up to 99%) characterised the estuary-marine transition and indicated progradation of RdlP sediments toward relict continental shelf sediments. This environment was also characterised by low marine organic matter determined by marine C/N values (c.a. 3) and a sharp decrease (c.a. between 75 and 90%) in C_{org}, N_t and $CaCO_3$ values. A sharp and systematic decrease in trace elements and the low Fe/Ca and Ti/Ca values elucidate the dominance of the marine influence in this region. The presence of the *B. elegantissima* assemblage, which includes typical marine shelf species and represents the highest ecological values (richness, diversity and density), indicates that this environment is characterised by more marine conditions.

The information reported in this paper is particularly important to better understand sedimentological dynamics in turbidity fronts of large estuaries and for elaborating more precise paleoenvironmental and palaeoceanographic reconstructions. A longer transect along the oriental channel from the upper river stations to full marine stations would increase our understanding of the signature and hydrodynamic control of this river–estuarine–marine transition system.

Acknowledgements

We would like to thank Mr. Edilson Faria from the Oceanographic Institute (IO-USP) for his help with sedimentological analyses in the laboratory. The oceanographic cruise was funded and supported by the Dirección Nacional de Recursos Acuáticos (DINARA). This paper is a contribution to the INQUA project 1202.

References

Adegbie, A.T., Schneider, R.R., Röhl, U., Wefer, G., 2003. Glacial millennial-scale fluctuations in central African precipitation recorded in terrigenous sediment supply and freshwater signals offshore Cameroon. Palaeogeography, Palaeoclimatology, Palaeoecology 197 (323–333) 1016/S0031-0182(03)00474-7.

Acha, E.M., Mianzan, H., Guerrero, R., Carreto, J., Giberto, D., Montoya, N., Carignan, M., 2008. An overview of physical and ecological processes in the Rio de la Plata estuary. Continental Shelf Research 28, 1579–1588.

Araujo, M.F., Jouanneau, J.-M., Valério, P., Barbosa, T., Gouveia, A., Weber, O., Oliveira, A., Rodríguez, A., Dias, J.M.A., 2002. Geochemical tracers of northern Portuguese estuarine sediments on the shelf. Progress of Oceanography 52 (2–4), 277–297.

Arz, H.W., Pätzold, J., Wefer, G., 1998. Correlated millennial-scale changes in surface hydrography and terrigenous sediment yield inferred from last-glacial marine deposits off northeastern Brazil. Quaternary Research 50, 157–166.

Ayup-Zouain, R.N., 2006. Evolución paleogeográfica y dispersión de los sedimentos del Rio de la Plata. In: Menafra, R., Rodriguez-Gallego, L., Scarabino, F., Conde, D. (Eds.), Bases para la Conservación y el Manejo de la Costa Uruguaya. Vida Silvestre Uruguay, Montevideo, pp. 1–8.

Boggs Jr., S., 2005. Principles of Sedimentology and Stratigraphy, fourth ed. Prentice Hall, New York, NY.

Bonetti, C., Eichler, B.B., 1997. Benthic foraminifera and thecamoebians as indicators of river/sea gradients in the estuarine zone of Itapitangui River—Cananéia/SP, Brazil. Anais da Academia Brasileira de Ciencias 69 (4), 545–563.

Botto, F., Gaitán, E., Mianzan, H., Acha, M., Giberto, D., Schiariti, A., Iribarne, O., 2011. Origin of resources and trophic pathways in a large SW Atlantic estuary: an evaluation using stable isotopes. Estuarine Coastal and Shelf Science 92 (1), 70–77.

Bray, J.R., Curtis, J.T., 1957. An ordination of the upland forest communities in southern Wisconsin. Ecological Monographs 27, 325–349.

Broecker, W.S., Peng, T.-H., 1982. Tracers in the Sea.. Lamont–Doherty Earth Observatory, Palisades N.Y..

Brönniman, P., Dias-Brito, D., Moura, J.A., 1981. Foraminíferos da fácies mangue da planície de maré de Guaratiba, Rio de Janeiro, Brasil, in: II Congresso Latino-Americano de Paleontologia, Anais, Porto Alegre, RS, pp. 877–891.

Burone, L., Pires-Vanin, A.M.S., 2006. Foraminiferal assemblages in the Ubatuba Bay, Southeastern Braziliancoast. Scientia Marina 70 (2), 203–217.

Burone, L., Venturini, N., Sprechmann, P., Valente, P., Muniz, P., 2006. Foraminiferal responses to polluted sediments in the Montevideo coastal zone, Uruguay. Marine Pollution Bulletin 52, 61–73.

Burone, L., Valente, P., Pires-Vanin, A.M.S., Sousa, S.H., de, M., Mahiques, M.M., Braga, E., 2007. Benthic foraminiferal variability on a monthly scale in a subtropical bay moderately affected by urban sewage. Scientia Marina 71 (4), 775–792.

Cabreira, A., Madirolas, A., Alvarez Colombo, G., Acha, E.M., Mianzan, H., 2006. Acoustic study of the Río de la Plata estuarine front. ICES Journal of Marine Science 63, 1718–1725.

Calvert, S.E., Fontugne, M.R., 2001. On the Late Pleistocene–Holocene sapropel record of climatic and oceanographic variability in the eastern Mediterranean. Paleoceanography 16, 78–94.

CARP, 1989. Estudio para la evaluación del Río de la Plata. Comisión Administradora del Río de la Plata. Buenos Aires, Montevideo, pp 422.

Cavallotto, J.L., 2002. Evolución Holocena de la Llanura costera del margen sur del Rio de la Plata. Revista de la Asociación Geológica Argentina, Buenos Aires 57 (4), 376–388.

Cavallotto, J.L., Violante, R.A., 2005. Rio de la Plata. In: de Barrio, R.E., et al. (Eds.), Relatorio Geología de la Provincia de Buenos Aires. XVI Congreso Geológico Argentino, La Plata, pp. 237–254.

Cazes-Boezio, G., Robertson, A.W., Mechoso, C.R., 2003. Seasonal dependence of ENSO teleconnections over South America and relationships with precipitation in Uruguay. Journal of Climate 16 (8), 1159–1176.

Clarke, K.R., Warwick, R.M., 2001. Change in Marine Communities: an Approach to Statistical Analysis and Interpretation. Plymouth Marine Laboratory, Plymouth.

Debenay, J.P., Geslin, E., Eichler, B.B., Duleba, W., Sylvestre, F., Eichler, P., 2001. Foraminiferal assemblages in a hypersaline lagoon Araruama (RJ) Brazil. Journal of Foraminiferal Research 31, 133–151.

Depetris, P.J., Kempe, S., Latif, M., Mook, W.G., 1996. ENSO-controlled flooding in the Paraná River (1904–1991). Naturwissenschaften 83, 127–129.

Diaz, R.J., Rosenberg, R., 1995. Marine benthic hypoxia: a review of its ecological effects and the behavioural responses of benthic macrofauna. Oceanography and Marine Biology Annual Review 33, 245–303.

Diaz, A.F., Studzinski, C.D., Mechoso, C.R., 1998. Relationships between precipitation anomalies in Uruguay and southern Brazil and sea surface temperature in the Pacific and Atlantic oceans. Journal of Climate 11 (2), 251–271.

Dymond, J.R., Suess, F., Lyle, M., 1992. Barium in deep-sea sediment: a geochemical proxy for paleoproductivity. Paleoceanography 7, 163–181.

Framiñan, M.B., Brown, O.B., 1996. Study of the Río de la Plata turbidity front Part I: Spatial and temporal distribution. Continental Shelf Research 16, 1259–1282.

Framiñan, M.B., Valle-Levinson, A., Sepulveda, H.H., Brown, O.B., 2008. Tidal variations of flow convergence, shear, and stratification at the Rio de la Plata estuary turbidity front. Journal of Geophysical Research 113, 1–17.

Frenz, M., Höppner, R., Stuut, J.-B.W., Wagner, T., Henrich, R., 2003. Surface sediment bulk geochemistry and grain-size composition related to the oceanic circulation along the South American continental margin in the Southwest Atlantic. In: Wefer, G., Mulitza, S., Ratmeyer, V. (Eds.), The South Atlantic in the Late Quaternary: Reconstruction of Material Budgets and Current Systems. Springer-Verlag, Berlin Heidelberg New York Tokyo, pp. 347–373.

Geyer, W.R., 1993. The importance of suppression of turbulence by stratification on the estuarine turbidity maximum. Estuaries 16 (1), 113–125.

Gibbs, R.J., Tshudy, D.M., Konwar, L., Martin, J.M., 1989. Coagulation and transport of sediment in the Gironde estuary. Sedimentology 36, 987–999.

Gilberto, D.A., Bermec, C.S., Acha, E.M., Mianzan, H., 2004. Large-scale spatial patterns of benthic assemblages in the SW Atlantic: the Rio de la Plata estuary and adjacent shelf waters. Estuarine Coastal Shelf Science 61, 1–13.

Goldberg, E., Arrhenius, G., 1958. Chemistry of pelagic sediments. Geochimica et Cosmochimica Acta 13, 153–212.

Gómez-Erache, M., Vizziano, D., Muniz, P., Nagy, G.J., 2001. The Health of the Río de la Plata system: Northerm Coast, Uruguay. In: Chopin, T., Wells, P.G. (Eds.), Opportunity and Challenges for Protecting, Restoring and Enhancing Coastal habitats in the Bay of Fundy. Proceedings of the Fourth Bay of Fundy Science Worshops, Saint John, New Brunswick. Environment Canada, Atlantic Region. Occasional Report No. 17, Environment Canada, Darmouth, Nova Scotia, pp. 17–35.

Govin, A., Holzwarth, U., Heslop, D., Ford Keeling, L., Zabel, M., Mulitza, S., Collins, J.A., Chiessi, C.M., 2012. Distribution of major elements in Atlantic surface sediments (36°N–49°S): imprint of terrigenous input and continental weathering. Geochemistry, Geophysics, Geosystems 13, Q01013 10.1029/2011gc003785.

Guerrero, R.A., Acha, E.M., Framiñan, M.B., Lasta, C.A., 1997. Physical oceanography of the Río de la Plata estuary, Argentina. Continental Shelf Research 17 (7), 727–742.

Gyllencreutz, R., Mahiques, M.M., Alves, D.V.P., Wainer, I.K.C., 2010. Mid- to late-Holocene paleoceanographic changes on the southeastern Brazilian shelf based on grain size records. The Holocene 20, 863–875.

Hori, K., Saito, Y., Zhao, Q., Cheng, X., Wang, P., Sato, Y., LI, C., 2001. Sedimentary facies of the tide-dominated paleo-Changjiang (Yangtze) estuary during the last transgression. Marine Geology 177, 331–351.

Hu, J., Peng, P., Jia, G., Mai, B., Zhang, G., 2006. Distribution and sources of organic carbon, nitrogen and their isotopes in sediments of the subtropical Pearl River estuary and adjacent shelf, Southern China. Marine Chemistry 98, 274–285.

Combes, Jacot Des, Caulet, H., Tribovillard, N. P., J.P., 1999. Pelagic productivity changes in the equatorial area of the northwest Indian Ocean during the last 400,000 years. Marine Geology 158, 27–55.

Combes, Jacot Des, Caulet, H., Tribovillard, N. P., J.P., 2005. Monitoring the variations of the Socotra upwelling system during the last 250 kyr: a biogenic and geochemical approach. Palaeogeography, Palaeoclimatology, Palaeoecology 223, 243–259.

Jaeger, J.M., Nittrouer, C.A., 1995. Tidal Controls on the formation of fine-scale sedimentary strata near the Amazon River mouth. Marine Geology 125, 259–281.

Jaeschke, A., Rühlemann, C., Arz, H., Heil, G., Lohmann, G., 2007. Coupling of millennial-scale changes in sea surface temperature and precipitation off northeastern Brazil with high-latitude climate shifts during the last glacial period. Paleoceanography 22, PA4206 10.1029/2006pa001391.

Jeffrey, S.W., Humphrey, G.F., 1975. New Spectrophotometric equations for determining chlorophylls a, b, c1 and c2 in higher plants, algae and natural phytoplankton. Biochemie und Physiologie Planzen 167, 191–194.

Kovach, W.L., 1999. MVSP. A Multivariate Statistical Package for Windows, ver. 3.1. Kovach Computing Services, Pentraeth, Wales.

Kruskal, J.B., Wish, M., 1978. Multidimensional Scaling. California Sage, Beverly Hills.

Kuramoto, T., Minagawa, M., 2001. Stable carbon and nitrogen isotopic characterization of organic matter in a mangrove ecosystem on the south-western coast of Thailand. Journal of Oceanography 57, 421–431.

Lick, W., Huang, H., 1993. Flocculation and the physical properties of flocs. In: Mehta, A.J. (Ed.), Nearshore and Estuarine Cohesive Sediment Transport. American Geophysical Union, Washington, DC, pp. 21–39.

Loeblich Jr., A.R., Tappan, H., 1988. Foraminiferal Genera and their Classification—PLATES, vol. 2. Van Nostrand Reinhold, New York.

Lopez-Laborde, J., 1987. Distribución de sedimentos superficiales de fondo en el Río de la plata exterior y plataforma adyacente. Investigaciones Oceanológicas 1, 19–30.

López-Laborde, J., Nagy, G.J., 1999. Hydrography and sediment transport characteristics of the Río de la Plata. In: Perillo, G.M.E., Pino, M., Piccolo, M.C. (Eds.), Estuaries of South America: Their Geomorphology and Dynamics. Springer-Verlag, Berlin, pp. 137–159. (Chapter 7).

Lorenzen, C.J., 1967. Determination of chlorophyll and phaeopigments: spectrophotometric equations. Limnology and Oceanography 12, 343–346.

Mahiques, M.M., Tessler, M.G., Ciotti, A.M., da Silveira, C.A., de Mello e Souza, S.H., Figueira, R.C.L., Tassinari, C.C.G., Furtado, V.V., Passos, R.F., 2004. Hydrodinamically driven patterns of recent sedimentation in the shelf and upper slope off Southeast Brazil. Continental Shelf Research 24, 1685–1697.

Mahiques, M.M., Wainer, I.E.K.C., Burone, L., Sousa, S.H.M., Silveira, I.C.A., Bícego, M.C., Alves, D.P., Hammer, O., 2009. A high-resolution Holocene record on the Southern Brazilian shelf: paleoenvironmental implications. Quaternary International 206, 52–61.

Mahiques, M.M., de Mello e Souza, S.H., Furtado, V.V., Tessler, M.G., de Lima Toledo, F.A., Burone, L., Figueira, R.C.L., Klein, D.A., Martins, C.C., Alves, D.P.V., 2010. The Southern Brazilian shelf: general characteristics, quaternary evolution and sediment distribution. Brazilian Journal of Oceanography 58 (special issue PGGM), 25–34.

Maksymowska, D., Richard, P., Piekarek-Jankowska, H., Riera, P., 2000. Chemical and isotopic composition of the organic matter sources in the Gulf of Gdansk (Southern Baltic Sea). Estuarine Coastal and Shelf Science 51, 585–598.

Martins, L.R., Martins, I.R., Urien, C.M., 2003. Aspectos sedimentares na plataforma continental na area de influência do Rio de La Plata. Gravel 1, 68–80.

Martins, V., Dubert, J., Jouanneau, J.-M., Weber, O., Ferreira da Silva, E., Patinha, C., Alverinho Dias, J.M., Rocha, F., 2007. A multyproxy approach of the Holocene evolution of shelf-slope circulation on the NW Iberian continental shelf. Marine Geology 239, 1–18.

Mechoso, C.R., Perez-Iribarren, G., 1992. Streamflow in southeastern South America and the Southern Oscillation. Journal of Climate 5 (12), 1535–1536.

Meyers, P.A., 1994. Preservation of elemental and isotopic source identification of sedimentary organic matter. Chemical Geology 114, 289–302.

Meyers, P.A., 1997. Organic geochemical proxies of paleoceanographic, paleolimnologic and paleoclimatic procceses. Organic Geochemistry 27 (5–6), 213–250.

Michener, R.H., Kaufman, L.S., 2007. Stable isotope ratios as tracers in marine food webs: an update. In: Lajtha, K., Michener, R.H. (Eds.), Stable Isotopes in Ecology and Environmental Science, second ed. Blackwell Publishing Ltd., pp. 238–278.

Milliman, J.D., Meade, R.H., 1983. World-wide delivery of river sediment to the oceans. Journal of Geology 91, 1–21.

Mori, P.E., Reeves, S.H., Correia, C.T., Haukka, M., 1999. Development of a fused glass disc XRF facility and comparison with the pressed powder pellet thechnique at Instituto de Geociências, São Paulo University. Revista Brasileira de Geociências 29 (3), 441–446.

Müller, A., Mathesius, U., 1999. The palaeoenvironments of coastal lagoons in the southern Baltic Sea, I. The application of sedimentary Corg/N ratios as source indicators of organic matter. Palaeogeography Palaeoclimatology Palaeoecology 145, 1–16.

Muller, A., Voss, M., 1999. The paleoenvironments of coastal lagoons in the southern Baltic Sea, II. $\delta^{13}C$ and $\delta^{15}N$ ratios of organic matter-sources and sediments. Palaeogeography, Palaeoclimatology, Palaeoecology 145, 17–32.

Muniz, P., Venturini, N., Pires-Vanin, A.M.S., Tommasi, L.R., Borja, A., 2005. Testing the applicability of a marine biotic index (AMBI) to assessing the ecological quality of soft-bottom benthic communities, in the South America Atlantic region. Marine Pollution Bulletin 50, 624–637.

Muniz, P., Venturini, N., Hutton, M., Kandratavicius, N., Pita, A., Brugnoli, E., Burone, L., García-Rodríguez, F., 2011. Ecosystem health of Montevideo coastal zone: a multi approach using some different benthic indicators to improve a ten-year-ago assessment. Journal of Sea Research 65, 38–50.

Murray, J.W., 2006. Ecology and Applications of Benthic Foraminifera. Cambridge University Press, Cambridge.

Nagy, G.J., Gómez-Erache, M., López, C.H., Perdomo, A.C., 2002. Distribution patterns of nutrients and symptoms of eutrophication in the Rio de la Plata estuary. Hydrobiologia 476, 125–139.

Nittrouer, C.A., Austin, J.A., Field, M.E., Kravitz, J.H., Syvitski, J.P.M., Wiberg, P.L., 2007. Continental Margin Sedimentation: From Sediment Transport to Sequence Stratigraphy. International Association of Sedimentologists. Blackwell Publishing Ltd..

Parker, G., Marcolini, S., Cavallotto, J.L., Violante, R.A., 1987. Modelo esquemático de dispersión de sedimentos en el Río de la Plata. Revista Ciencia y Tecnología del Agua (Santa Fe, Argentina) 1 (4), 68–80.

Parker, G., Violante, R.A., 1993. Río de la Plata y regiones adyacentes. In: Iriondo, M. (Ed.), El Holoceno en la Argentina, Vol. 2. CADINQUA, pp. 163–230.

Paytan, A., Kastner, M., Martin, E.E., MacDougall, J.D., Herbert, T., 1993. Marine barite as a monitor of seawater strontium isotope composition. Nature 366, 445–449.

Paytan, A., Kastner, M., 1996. Benthic Ba fluxes in the central Equatorial Pacific, implications for the oceanic Ba cycle. Earth and Planetary Science Letters 142, 439–450.

Pfeifer, K., Kasten, S., Hensen, C., Schulz, H.D., 2001. Reconstruction of primary productivity from the barium contents in surface sediments of the South Atlantic Ocean. Marine Geology 177, 13–24.

Pisciottano, G., Díaz, A., Cazes, G., Mechoso, C.R., 1994. El NIÑO–Southern Oscillation impact on rainfall in Uruguay. Journal of Climate 7 (8), 1286–1304.

Piola, A.R., Campos, E.J.D., Moller Jr, O.O., Charo, M., Martinez, C., 2000. Subtropical shelf front off eastern South America. Journal of Geophysical Research 105, 6565–6578.

Prahl, F.G., Ertel, J.R., Goni, M.A., Sparrow, M.A., Eversmeyer, B., 1994. Terrestrial organic carbon contributions to sediments on the Washington margin. Geochimica et Cosmochimica Acta 58, 3035–3048.

Prakash Babu, C., Brumsack, H.J., Schnetger, B., Bottcher, M.E., 2002. Barium as a productivity proxy in continental margin sediments: a study from the eastern Arabian Sea. Marine Geology 184, 189–206.

Rabalais, N.N., Turner, R.E., Justic, D., Dortch, Q., Wiseman Jr., W.J., Sen Gupta, B.K., 1996. Nutrient changes in the Mississippi River and system responses on the adjacent continental shelf. Estuaries 19, 386–407.

Robertson, A.W., Mechoso, C.R., 1998. Interannual and decadal cycles in river flows of southeastern South America. Journal of Climate 11 (10), 2570–2581.

Rodriguez-Graña, L., Calliari, D., Conde, D., Sellanes, J., Urrutia, R., 2008. Food web of a SW Atlantic shallow coastal lagoon: spatial environmental variability does not impose substantial changes in the trophic structure. Marine Ecology progress Series 361, 69–83.

Romero, O.E., Hensen, C., 2002. Oceanographic control of biogenic opal and diatoms in surface sediments of the Southwestern Atlantic. Marine Geology 186, 263–280 10.1016/S0025-3227(02)00210-4.

Saito, Y., Nishimura, A., Matsumoto, E., 1989. Transgressive sand sheet covering the shelf and upper slope off Sendai, Northeast Japan. Marine Geology 89, 245–258.

Scott, D.B., Medioli, F.S., Schafer, C.T., 2001. Monitoring of Coastal Environments Using Foraminifera and Thecamoebian Indicators. Cambridge University Press, United Kingdom.

Shannon, C.E., Weawer, W., 1963. The Mathematical Theory of Communication. The University of Ilinois Press, Urbana.

Stein, R., 1991. Accumulation of organic carbon in marine sediments. Results from the Deep Sea Drilling Project/Ocean Drilling Program. Lecture Notes in Earth Sciences, 34. Springer, Berlin 217p.

Strickland, J.D.H., Parsons, T.R., 1972. A practical handbook of sea water analysis. Fisheries Research Board Of Canada—Bulletin 167, 207–211.

Syvitski, J.P.M., Peckham, S.D., Hilberman, R.D., Mulder, T., 2003. Predicting the terrestrial flux of sediment to the global ocean: a planetary perspective. Sedimentary Geology 162, 5–24.

Traykovski, P., Geyer, R., Sommerfield, C., 2004. Rapid sediment deposition and fine-scale strata-formation in the Hudson estuary. Journal of Geophysical Research, 109, http://dx.doi.org/10.1029/2003JF000096.

Tyson, R.V., 1995. Sedimentary Organic Matter. Organic Facies and Palynofacies.

Urien, C.M., 1967. Los sedimentos modernos del Río de la Plata. Boletin SHIN 4 (2), 113–213.

Urien, C.M., Ewing, M., 1974. Recent sediments and environment of Southern Brazil, Uruguay, Buenos Aires, and Rio Negro continental shelf. In: Burk, C., Drake, C.H. (Eds.), The Geology of Continental Margins. Springer-Verlag, New York, pp. 157–177.

Urien, C.M., Martins, L.R., Martins, I.R., 1980. Evolução geológica do Quaternário do litoral atlântico uruguaio, plataforma continental e regiões vizinhas. CECO/URFGS, Notas Técnicas 3, 7–43.

Violante, R.A., Parker, G., 2004. The post-last glacial maximum transgression in the de la Plata River and adjacent inner continental shelf, Argentina. Quaternary International 114, 167–181.

Wada, E., Hattori, A., 1991. Nitrogen in the Sea: Forms, Abundances, and Rate Processes. CRC Press, Boca Raton, FL.

Walton, W.R., 1952. Techniques for recognition of living foraminifera. Contribution of Cushman Foundation—Journal of Foraminiferal Research 3, 56–60.

Walton, W.R., Sloan, B., 1990. The genus *Ammonia* Brünnich. 1972: its geographic distribution and morphological variability. Journal of Foraminiferal Research 20, 128–156.

Wei, G., Liu, Y., Li, X., Chen, M., Wei, W., 2003. High-resolution elemental records from the South China Sea and their paleoproductivity implications. Paleoceanography, 18, http://dx.doi.org/10.1029/2002PA000826.

Wellershaus, S., 1981. Turbidity maximum and mud shoaling in the Weser estuary; Archive. Hydrobiology 92, 161–198.

Zaninetti, L., Brönnimann, P., Dias-Brito, D., Arai, M., Casaletti, P., Koutsoukos, E., Silveira, S., 1979. Distribution écologique dês foraminifères dans La mangrove d'Acupe, État de Bahia, Brésil. Notes Du Lab. De Paléontol. Univ. Genève 4, 1–17.